Hyperthermia Ablation of Breast Tumors Using Ultrasound

BEE 4530 – Computer-Aided Engineering: Applications to Biomedical Processes

May 9, 2014

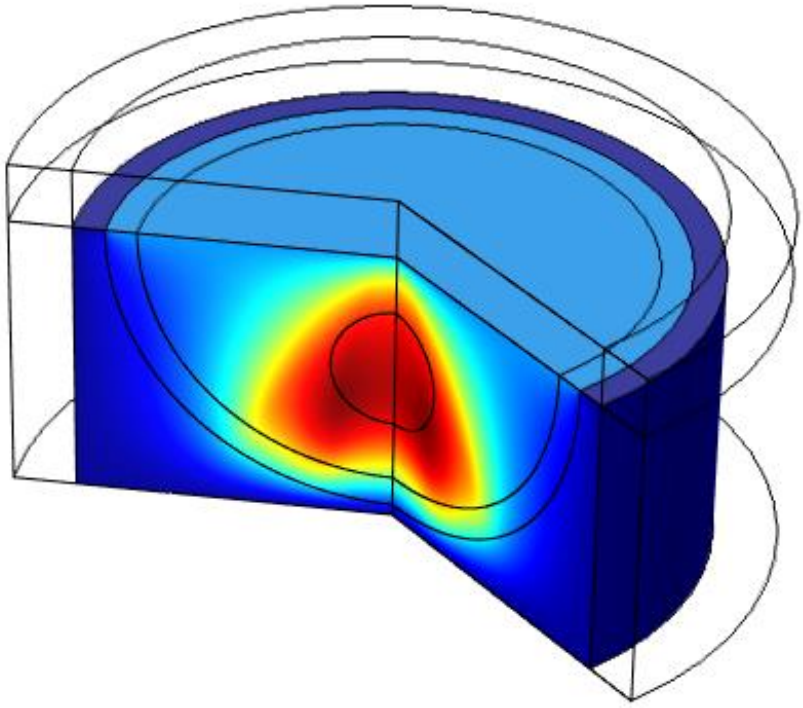

Group 4
Shiyi Jin
Xing Wang
Mona Yuan
Anqi Zheng

Table of Contents

Executive Summary

Breast cancer is the most prevalent type of cancer, excluding lung cancer, for women in the United States. Left untreated, a malignant primary tumor in the breast can metastasize via the underarm lymph nodes, increasing risk of death. Invasive surgery techniques such as mastectomy and lumpectomy are used to treat breast cancer. Although breast-conserving therapies are successful in tumor removal, these surgeries still involve radical resection of the tumor, postoperative radiotherapy, and undesirable cosmetic effects.

More recently, less invasive techniques such as cryotherapy and hyperthermia have gained wide appeal. One hyperthermia technique, radiofrequency ablation (RFA), delivers high-frequency alternating currents to heat tissue. This technique minimizes pain, avoids infections and scar formations, and reduces recovery time. However, RFA still requires a needle-like probe to be inserted directly into the breast to deliver heat.

In contrast to open surgery and RFA techniques, ultrasound hyperthermia is the only non-invasive technique that does not require any incisions or percutaneous insertions. Ultrasound hyperthermia uses focused ultrasound waves to destroy targeted tissue. During this procedure, an ultrasound transducer delivers mechanical energy to tissues, resulting in temperature increase and thus cell death. Magnetic resonance imaging can be used to guide this non-invasive treatment, eliminating the need to insert a probe. Possible side effects of the procedure include local pain, skin burns, and sometimes injury to surrounding tissue.

Our goal is to use COMSOL to model an ultrasound hyperthermia treatment of a breast tumor using a 2D axisymmetric geometry. By modeling the acoustic pressure field in the breast and surrounding water, we will determine the optimum combination of applied frequency and time to reach 42-45 °C for tumor destruction while minimizing damage to surrounding tissues. A frequency of 1 MHz will be used as a starting point, for which tissue properties are best defined.

Introduction

A woman in the U.S. today has about a one in eight chance of developing invasive breast cancer during her lifetime. It was estimated that 192,370 women and 1,910 men in the United States were diagnosed with breast cancer in 2009, and an approximate 40,610 of those affected died as a result of breast cancer [1]. Breast cancer death rates exceed that of all cancer, with the exception of lung cancer, for women in the U.S [1].

The uncontrolled growth of cancerous breast cells causes formations of malignant tumors that can spread to other parts of the body via the underarm lymph nodes. Traditional treatment of breast cancer involves invasive surgery, such as mastectomy and lumpectomy [2]. Mastectomy, the removal of entire breast tissues, was the single most popular therapy since its introduction in 1894 until breast-conserving lumpectomy became common in the 1970s [3]. Though less invasive, these breast-conserving therapies still require radical resection of the tumor, postoperative radiotherapy, and produced undesirable cosmetic results [4].

Hyperthermia for Breast Tumor Treatment

Advancements in technology over recent years have allowed significant development in treatments of breast cancer. While early attempts of hyperthermia treatment resulted in unintended normal tissue injuries, newer tools today have allowed more precise and better controlled heat delivery for tumor ablation. As a result, alternative minimally invasive techniques such as cryotherapy and hyperthermia have recently garnered wide appeal [2].

Radiofrequency ablation (RFA) is one example of a widely applied hyperthermia treatment in clinical practice. In 1999, the application of thermal energy caused by high-frequency alternating currents was reported to successfully ablate local breast tissue with improved cosmetic results. The controlled delivery of electrical energy allowed tumor temperature to rise above 100 ℃ within 10 to 20 minutes [4]. Similar to other minimally invasive therapies, RFA minimizes pain, avoids infections and scar formations, and reduces recovery time [3]. However, RFA and many minimally invasive therapies require an image-guided insertion of a needle-like probe directly into the breast to deliver heat [3].

Ultrasound Hyperthermia Therapy for Tumor Ablation

Ultrasound hyperthermia therapy, an emerging method for destroying tumor tissue, eliminates the need to make incisions or percutaneous insertions into the breast. Ultrasound hyperthermia therapy uses focused ultrasound waves to destroy tissue. A transducer placed near the skin surface delivers mechanical energy that tissues absorb, resulting in temperature increase and thus cell death [5]. A coupling agent such as water is used to propagate the acoustic waves and cool normal tissue. This application can be used to destroy tumors in prostate [6] and breast cancers [7], among others.

In mild ultrasound hyperthermia therapy, tumors are exposed to low-intensity ultrasound for long periods of time (10-60 minutes) in order to maintain a temperature needed for

ablation. In another approach termed “high intensity focused ultrasound” or HIFU, high intensity ultrasound waves propagate into the tissue rapidly for several seconds (0.1-30s) to rapidly increase the temperature of the tumor [8]. During the procedure, magnetic resonance imaging (MRI) can be used as a way to guide HIFU treatment because of its high resolution when imaging soft tissue. Currently, MR guided-HIFU can play a role in pre-treatment planning, treatment monitoring, and post treatment evaluation [9].

Ultrasound hyperthermia treatment is preferred by some patients because it is minimally invasive and can be performed as an outpatient procedure with few side effects and fast recovery time. Possible side effects include local pain in the exposed site, skin burns, and in more severe cases injury to the surrounding tissue. Currently, ultrasound hyperthermia is in the clinical trials stages of development. However, advancements in research may allow this to become a more commonly used treatment in the future [10].

Problem Statement and Design Objectives

We used COMSOL to model breast tumor ablation by ultrasound to find the optimal applied duration at various frequencies. The goal is to reach a tumor temperature of 42-45 ℃, which is high enough to destroy cancerous cells, while minimizing damage to surrounding tissues [11, 12].

We used the Helmholtz equation for linear acoustic wave propagation to model the acoustic pressure field in the water and tissue domains. The pressure field solution was used to determine the volumetric rate of acoustic heat generation, which was used to model heat transfer in the water and tissue domains.

Schematic of COMSOL Model with Boundary Conditions.

The figure below indicates the relative size and geometry of the tumor, breast, water domain, and transducer in our initial model. Boundary and initial conditions have also been labeled.

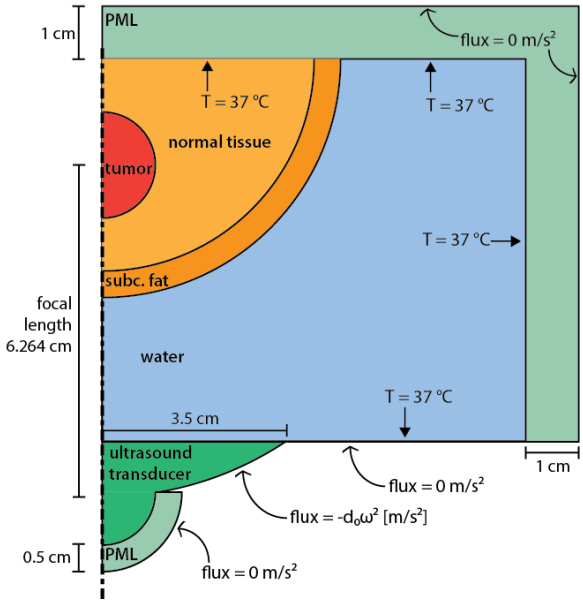

Figure 1. Schematic of initial 2D axisymmetric model of hemispherical breast with spherical tumor. Boundary conditions for the pressure field and temperature for heat transfer are included. Flux at the axisymmetric boundary is 0 for both temperature and pressure.

The initial and boundary water temperatures were later varied in optimization. Additionally, the height of the water domain was changed in order to better focus the heating effect on the region of the tumor. Figure 2 illustrates the geometry used in our optimized model.

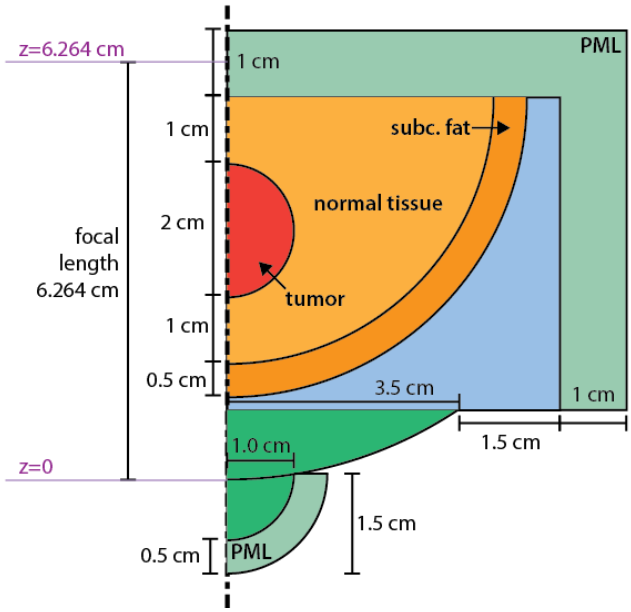

Figure 2. Schematic of the 2D axisymmetric model used in optimization. This includes a smaller water domain.

Heat Transfer Model

The tumor tissue was modeled as a sphere of diameter 2 cm at a depth of 1.5 cm below the surface of the skin [13, 14]. We will incorporate the effect of ultrasound as a volumetric acoustic heat source which will be used in the governing equation:

$$\rho C_p \frac{\partial T}{\partial t} = \nabla \cdot (k \nabla T) + Q \tag{1}$$

where T is the temperature, ρ is the density, C_p is the specific heat, k is the thermal conductivity and Q is the acoustic heat source. Blood perfusion and metabolic heat generation in the tissue will be neglected.

Water will be used to propagate ultrasound waves. The water boundaries will be assumed to be far away at water temperature of 37 ℃ [15]. Boundary conditions at the bottom edge of the tissue model will be assumed to be far away at body temperature of 37 ℃. At the axis of symmetry, temperature flux is equal to zero. The initial condition is a temperature of 37 ℃ for tumor, tissue, and water.

Numerical Model for Ultrasound Pressure and Heat Generation

We will use the homogeneous Helmholtz equation in 2D axisymmetric cylindrical coordinates to model the sound pressure from the acoustic source:

$$\frac{\partial}{\partial r}\left[-\frac{r}{p_c}\left(\frac{\partial p}{\partial r}\right)\right] + r\frac{\partial}{\partial z}\left[-\frac{1}{p_c}\left(\frac{\partial p}{\partial z}\right)\right] - \left[\left(\frac{\omega}{c_c}\right)^2\right]\frac{rp}{p_c} = 0 \tag{2}$$

where r and z are the radial and axial coordinates, p is the acoustic pressure, and ω is the angular frequency. The density, ρ_c, and the speed of sound, c_c, are complex-valued to account for the material's damping properties [8].

The Helmholtz equation is used under the assumption that the acoustic wave propagation is linear and that the amplitudes of shear waves are much smaller than that of the pressure waves. Nonlinear effects and shear waves are therefore neglected.

The boundary conditions are no flux (no acceleration) at all boundaries except for the outer boundary of the bowl of the transducer (Figure 1). The flux at the edge of the transducer is an acceleration condition of $-d_0\omega^2$, where d_0 is the displacement amplitude of the transducer and $\omega = 2\pi f$ where f is the ultrasound frequency [8]. This acceleration term represents the surface intensity.

Perfectly matched layers were used at the edge of the transducer and the tissue and water domains to model the absorption of pressure waves and eliminate their reflection from the boundaries.

Q, the volumetric acoustic heat source, will be calculated as:

$$Q = 2\alpha I = 2\alpha \left| Re\left(\frac{1}{2} p\boldsymbol{v}\right)\right| \quad (3)$$

where α is the acoustic absorption coefficient, I is the magnitude of the acoustic intensity, p is the acoustic pressure, and v is the acoustic particle velocity vector [8, 16].

The acoustic absorption coefficient α was assumed to be equal to the attenuation coefficient of the tissue and water. This was implemented as a function of frequency:

$$\alpha = \alpha_0 f^n$$

where α_0 and n were found in literature (see Appendix A for specific definitions).

The same properties were implemented for tumor, normal tissue, and fat in the tissue domain.

Results

Preliminary Solutions for Pressure and Heat Generation

The model was first run at 1 MHz and an initial water bath temperature of 37 ºC for 15 minutes as a reference point. This was done to see where the greatest pressure field and temperature change would be located; therefore, this plot would indicate whether or not heating was focused and sufficient. Shown below are the surface plot results of the pressure field and temperature (Figures 3 and 4). The pressure field was focused at the tumor (Figure 3).

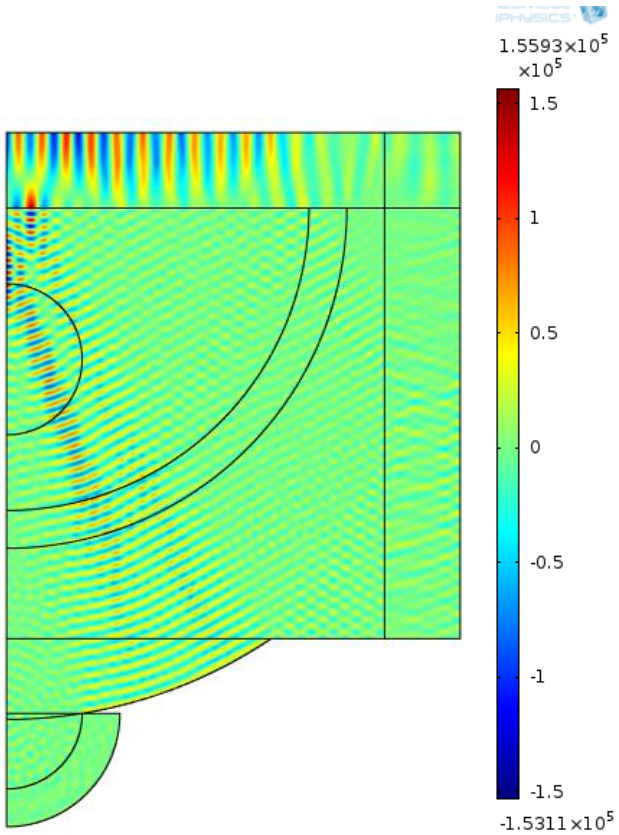

Figure 3. Surface plot of pressure solution, with an ultrasound frequency of 1 MHz. The focal point of the pressure field appears to be at the top of the domain, near the edge of the perfectly matched layer.

There was focused heating at the tumor but the maximum 2.8 ºC rise in temperature was insufficient for tumor ablation (Figure 4).

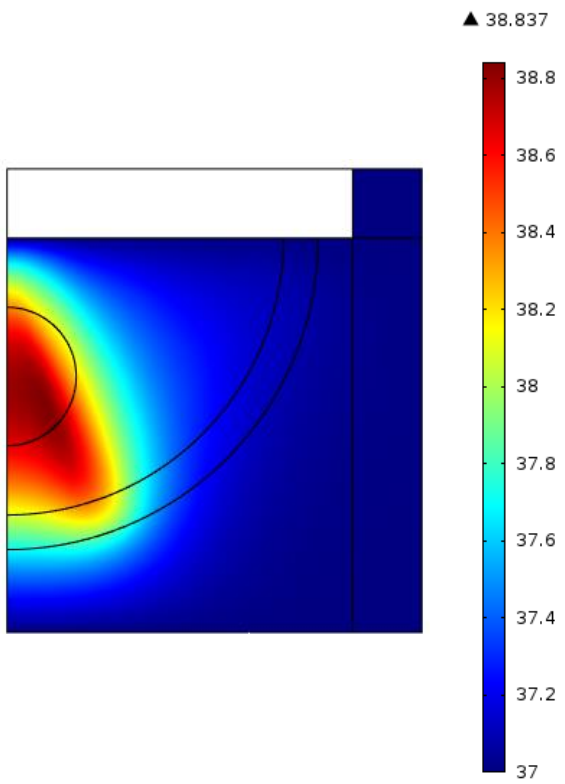

Figure 4. Surface plot of temperature (ºC) at time 900s (15 minutes) with an ultrasound frequency of 1 MHz.

Figure 4 indicates that the majority of heating occurs near the center of the tumor (after an adjustment to our geometry). Maximum temperature was raised about 2.8 °C, which is not yet sufficient for tumor destruction, but the temperature effect is focused on the tumor.

In addition, temperature vs. time of three different points was plotted to see how different regions of the tissue vary in temperature change (Figure 5). The temperature at point 1, the tumor center, was raised 1.8 °C from the initial 37 °C by the end of heating at 900 s. The temperature at point 2 in the normal tissue was raised about 0.4 °C. It is notable that the temperature at point 3 was raised almost 1.7 °C as well; this is due to the effect of the ultrasound focusing approximately along the line formed by points 1 and 3 (Figure 3).

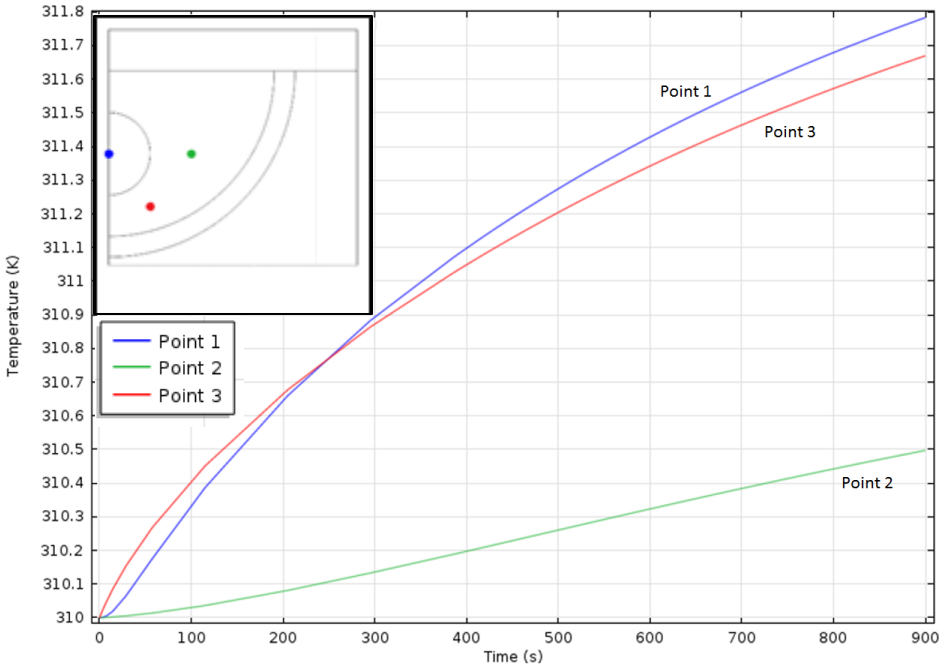

Figure 5. Temperature over time at 3 locations in the tumor: the center of the tumor (point 1), and two points in the normal tissue (points 2 and 3).

These preliminary results for temperature at various points in the tissue indicate that normal tissue damage is a result we must take into account during the ultrasound hyperthermia treatment, because some points in the normal tissue will heat at approximately the same rate as the tumor. Optimization of the initial water temperature and frequency later performed takes normal tissue damage into account.

A surface average temperature of the tumor was also evaluated to quantify roughly how much the tumor heated up using the given parameters (Figure 6).

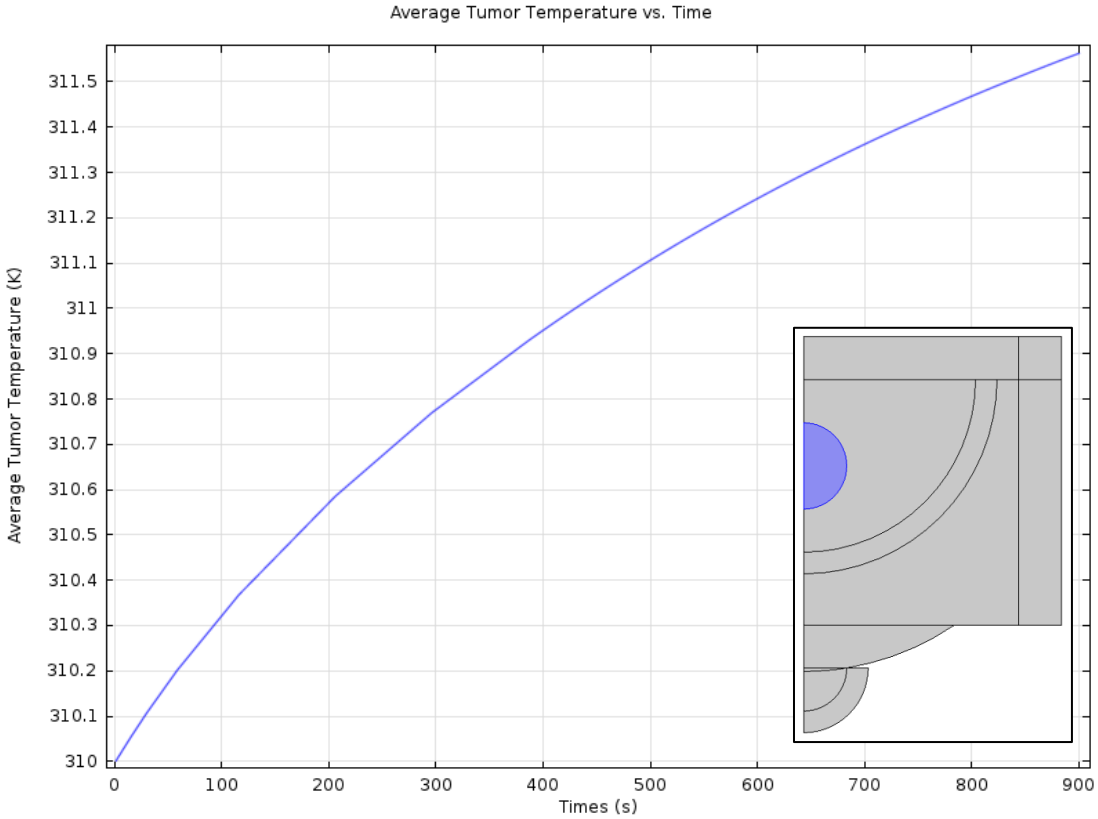

Figure 6. Average temperature in the tumor vs. time with an ultrasound frequency of 1 MHz. The tumor is shown in the inset.

It can be seen that average tumor temperature reaches about 38.5 ºC, which is not yet high enough for thermal destruction of the tumor tissue. Furthermore, the average tumor temperature is not necessarily indicative of the complete success of the hyperthermia therapy. The surface plot of temperature (Figure 4) indicates that heating within the tumor is not uniform, as some areas of the tumor will reach higher temperatures than others; this means that while the average temperature of the tumor may be high, areas of the tumor tissue may still remain intact and undamaged. Thus, in our optimization, we evaluated the fraction by volume of tumor that reached a certain temperature for tissue destruction, rather than an average temperature.

In order to increase heating effects, a preliminary model at 3 MHz was also run (Figure 7). Maximum temperature was raised about 14.3 ºC; however, the maximum temperature occurs in the normal breast tissue instead of in the tumor. Therefore, the heating is not focused on the tumor with an increase in frequency. This justified the need to change the geometry in order to focus the heating effect on the tumor. The new geometry, which decreased the water domain's height by 1 cm, was implemented in the model used in optimization.

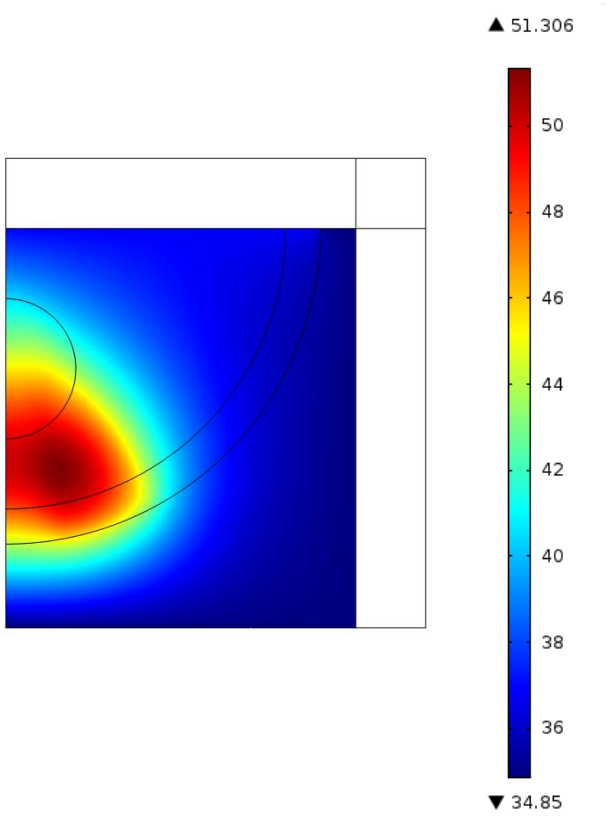

Figure 7. Surface plot of temperature at time 900 seconds (15 minutes) with an ultrasound frequency of 3 MHz.

Optimization of Frequency and Initial Water Temperature

Principles for Optimization

In order to determine the best combination of frequency and initial (and boundary) water temperature, an optimization process was developed.

We sought to find the conditions where, in order of priority:

1. All of the tumor was destroyed, by raising the entire tumor volume above 42 °C.
2. As little of the normal tissue and fat were destroyed as possible, by keeping as much of the volume of normal tissue and fat below 42 °C.
3. The heating time was minimized.

Because the goal of the treatment is to destroy tumor tissue, the first requirement that 100% of the tumor tissue is destroyed by heating above 42 °C must be met. The requirement that all tumor tissue be destroyed corresponds to the standard goal of negative margins (complete removal of tumor plus some removal of normal breast tissue) in current surgery practices for breast cancer [17].

The next important requirement is the second one, because we seek to minimize damage to normal tissues. Because the longer the heating time, the more damage (heating) to the normal tissue, the third requirement that time be minimized was taken into account by choosing the first time point that all tumor tissue reached 42 °C.

Optimization Process

By evaluating integrals for the volume of tumor tissue and normal tissue that had reached temperatures of 42 °C, it was possible to determine the conditions under which the entire tumor was destroyed while damaging the minimum amount of normal tissue. Frequencies between 1.5 MHz and 3.5 MHz were tested, along with combinations of initial water temperatures ranging from 10 °C to 35 °C.

The fraction of normal tissue damaged at the earliest time that 100% of the tumor reached 42 °C at each frequency and initial water temperature combination is plotted in Figure 8. From this plot, we can visualize which combination of parameters would result in the lowest amount of normal tissue damage.

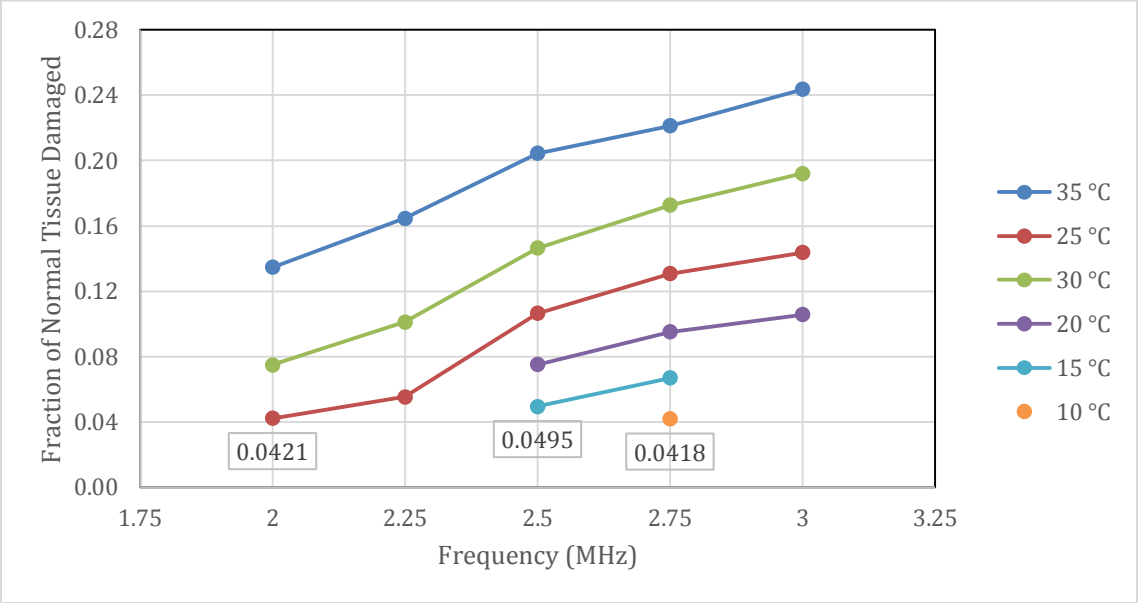

Figure 8. Fraction of normal tissue damaged at the earliest time that 100% of the tumor reached 42 °C, plotted against frequency, at various initial water temperatures. Any frequency/initial water temperature combination that did not achieve 100% tumor damage after 15 minutes were not plotted. The three best conditions are labeled with their fraction of normal tissue damaged for comparison.

It should be noted that frequencies of 1.5 MHz and 3.5 MHz resulted in incomplete heating of the tumor to the destruction temperature of 42 °C, and several other combinations of frequency and initial water temperature also did not achieve complete heating of the tumor.

This incomplete heating of tumor at low frequencies such as 1.5 MHz resulted from the fact that the ultrasound intensity (or pressure) at the tumor was not high enough to result in sufficient heating of the tumor, at any initial water temperature, similar to our earlier observations from lower frequencies such as 1 MHz. Figure 9 provides an illustration of the insufficient heating at the frequency of 1.5 MHz.

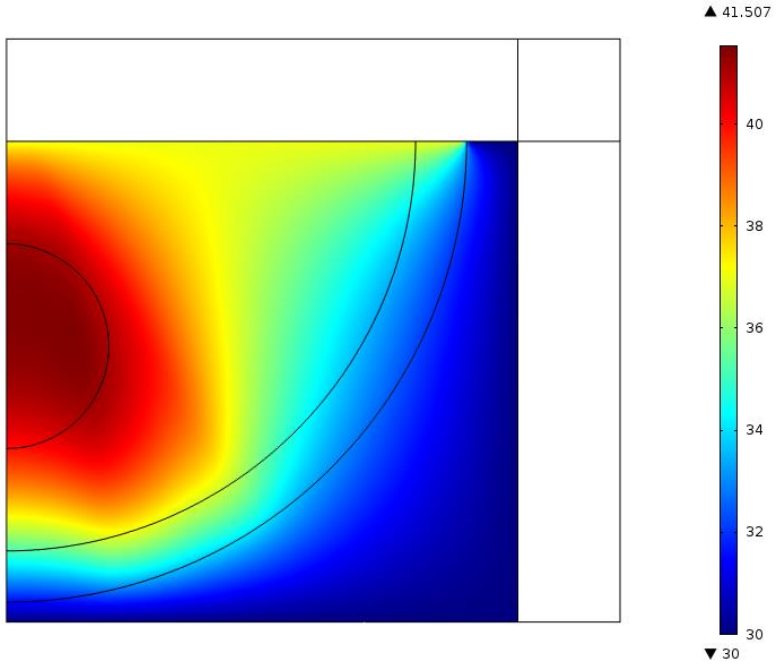

Figure 9. Surface plot of temperature at 1.5 MHz, with initial water temperature 30 °C. The maximum temperature achieved was 41.5 °C, which was insufficient for tissue destruction.

In contrast, at high frequencies such as 3.5 MHz, the effect of heating from acoustic waves decreased as waves traveled further into the water and tissue domains. This is because the property of attenuation was implemented to increase as frequency increased. Thus, the pressure waves were greatly attenuated when they reached the depth of the tumor within the tissue (Figure 10), and the region of highest pressure oscillations did not match the area of the tumor.

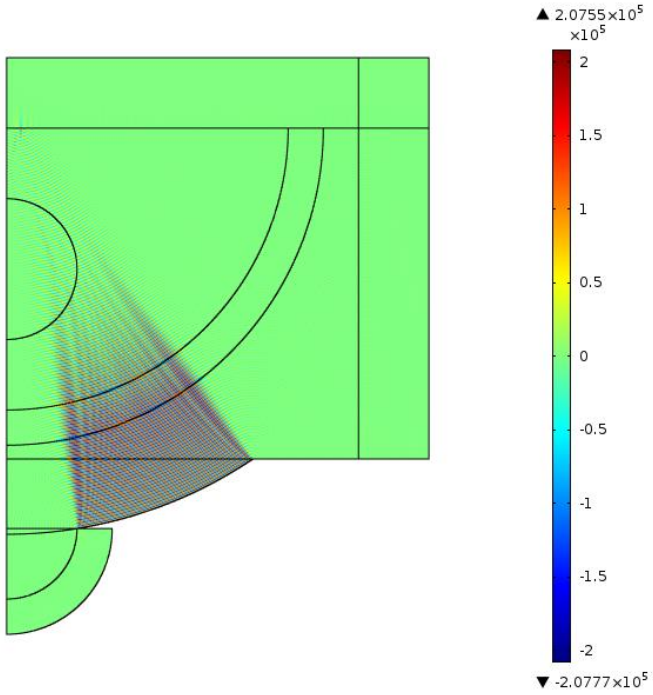

Figure 10. Pressure surface plot for 3.5 MHz frequency, illustrating effects of acoustic wave attenuation at high frequencies.

For the 3.5 MHz model, the heating was still focused primarily at the tumor (Figure 11). Despite the lack of focusing of the pressure waves, this focusing of heating can be attributed to the fact that the water cools the fat and normal tissue at the edge of the domain, leading to cooling at the region where pressure oscillations were the greatest.

The combined effect of the pressure attenuation and the cooling effect of water is an overall lower temperature increase. As can be seen in Figure 11, the highest temperature reached was 41.5 °C (with an initial water temperature of 30 °C), which is again insufficient for tumor ablation.

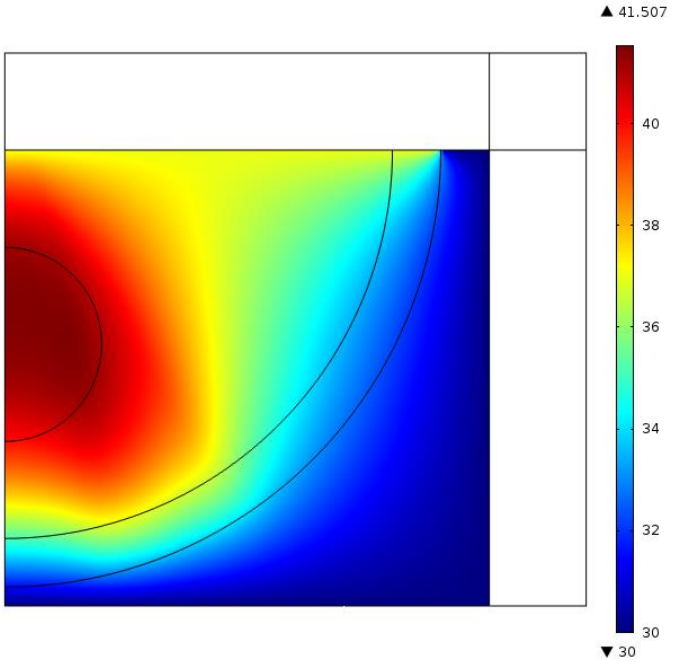

Figure 11. Temperature surface plot for 3.5 MHz. An initial water temperature of 30 °C and a time of 900 seconds (15 minutes) is shown for this temperature surface plot.

The optimization results for low and high ultrasound frequencies demonstrate that only a certain range of frequencies can be used to ensure sufficient heating to the tumor.

Results for Optimized Conditions

We found that the lowest amount of normal tissue damage occurred with an ultrasound frequency of 2.75 MHz and an initial water temperature of 10 °C, at a time of 900 seconds, or 15 minutes. (Results for the volume of normal tissue damage at each frequency and initial water temperature are included in Appendix C.) The surface intensity was 9188 W/m^2.

The surface plot at 15 minutes (Figure 12) indicates that most of the heating occurred in the tumor, although some breast tissue was also damaged. By this time, 100% of the tumor had reached a temperature of 42 °C, while 4.18% (7.81 cm^3) of the breast tissue was damaged.

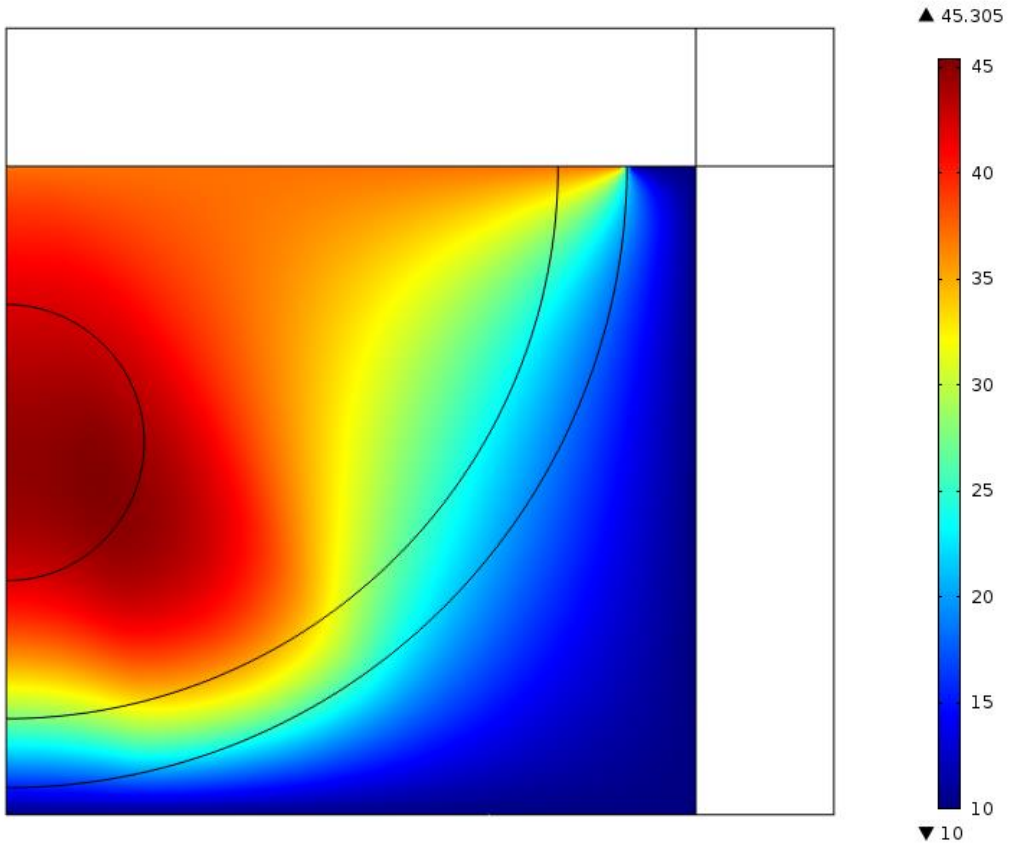

Figure 12. Surface plot of temperature (°C) in breast and water domains at a frequency of 2.75 MHz with initial water temperature 10 °C at time 900 seconds (15 minutes). This combination of frequency and initial water temperature was optimal for tumor destruction while maintaining normal breast tissue and fat.

The tumor tissue reaches an average of 44.2 °C by 900 seconds of heating (Figure 13), which is an indication that the tumor temperature is generally within the 42 to 45 °C range needed for hyperthermia ablation.

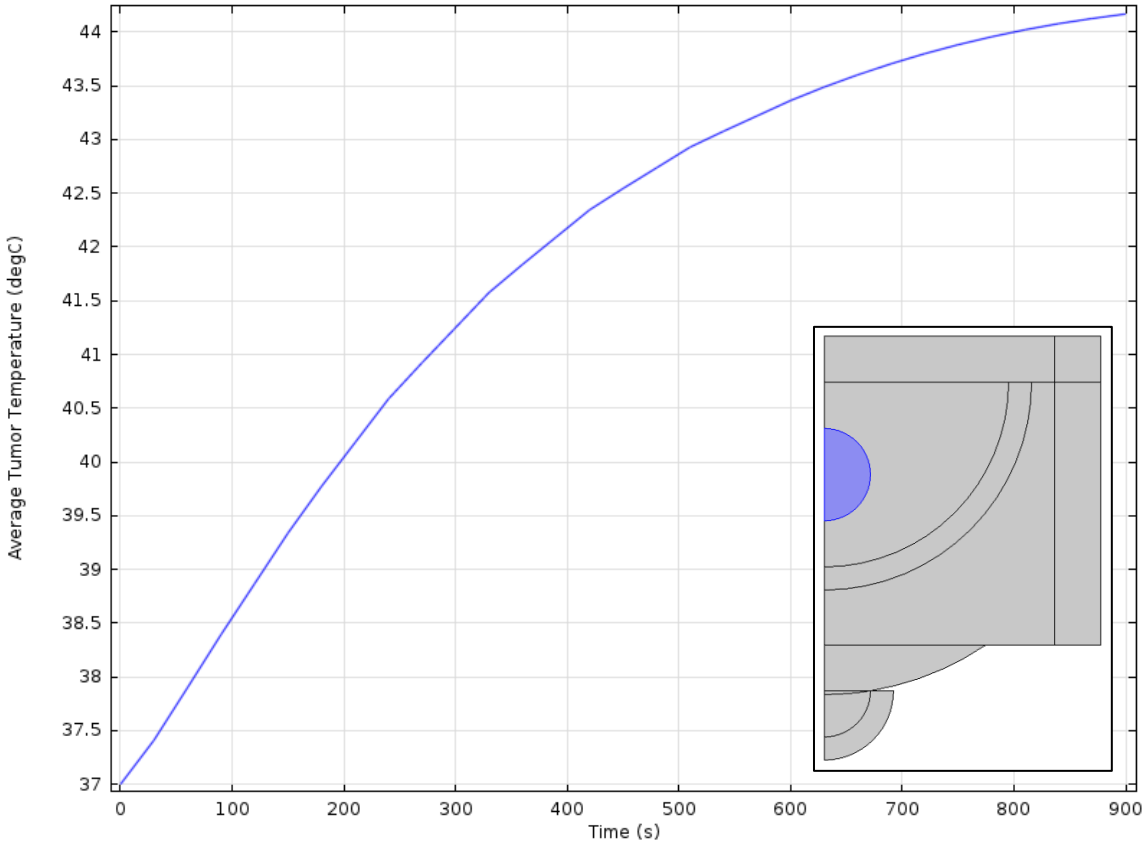

Figure 13. Average temperature in tumor (blue in inset) over time for a frequency of 2.75 MHz and an initial water temperature of 10 °C. At the time of 900 seconds (15 minutes), the average tumor temperature was 44.2 °C.

Sensitivity Analysis

Thermal conductivity, specific heat capacity, density, and attenuation coefficient of water and tissue were each varied by ±10% and ±20% while keeping all other parameters constant. This ±10% and ±20% difference from the middle value allows each of these parameters to fall between literature values in the temperature ranges we were interested in, from 30 ºC to 50 ºC [16, 18-22]. The middle value used included all properties of water evaluated at 37 ºC [16, 18, 19] and tissue properties obtained from literature [8]. For these parameters, frequency was set at 2.25 MHz and initial water temperature at 25 ºC. In addition, the constant flux surface intensity term from the transducer was changed by ±10% and ±20% and used as another parameter for sensitivity analysis.

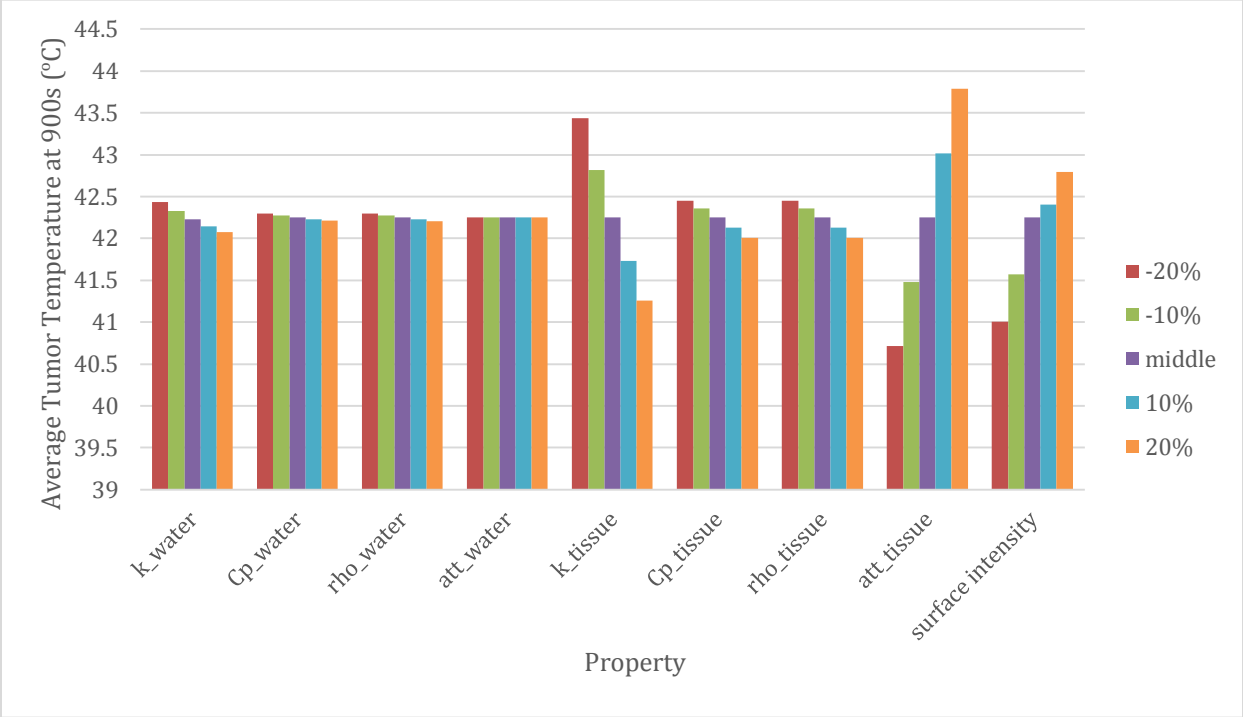

Figure 14. The thermal conductivity, specific heat, density of both water and tissue as well as surface intensity of the transducer were changed by increasing and decreasing by 10% and 20% from the middle values.

Average tumor temperature was least sensitive to the water's thermal conductivity, specific heat, density, and attenuation as shown in Figure 6. For these parameters, the average tumor temperature varied less than 0.5 ºC from the highest to the lowest values. This is due to the fact that little heating occurred in the water domain, which was used as a coolant. In addition, average tumor temperature was fairly constant with changes in specific heat and density of tissue as well.

Our model was most sensitive to thermal conductivity and attenuation in the tissue, as well as surface intensity. For these parameters, the average tumor temperature varied from 2-3 ºC. The tissue is a more conductive material than water, and there is more thermal heating in the tissue in general, especially in the tumor domain. Therefore, more

accurate and precise properties for thermal conductivity in tissue would achieve more accurate results.

Attenuation and surface intensity of the transducer both depend on frequency. It was expected that frequency has a greater effect on heating because of its significance in the pressure field equation. It is important to note that frequency was a parameter used to optimize our model. From the results shown in Figure 14, we can conclude that frequency, surface intensity and attenuation play a large role in the heating of breast tumors.

Accuracy Check: Comparison with Numerical Model of Ultrasound Hyperthermia of Breast Tumor

To verify our model, we compared it to an *in vivo* experiment of tissue phantom heating [23].

The experiment used an embedded thermocouple to measure the temperature at the focus for a 2.6 cm diameter vessel. A blood simulant and an axially symmetric tissue phantom (10.72-cm diameter, 8-cm length) were used. The temperature was measured after an insonation time of 5s using a frequency of 1.0 MHz and flow velocity of 0 cm/sec.

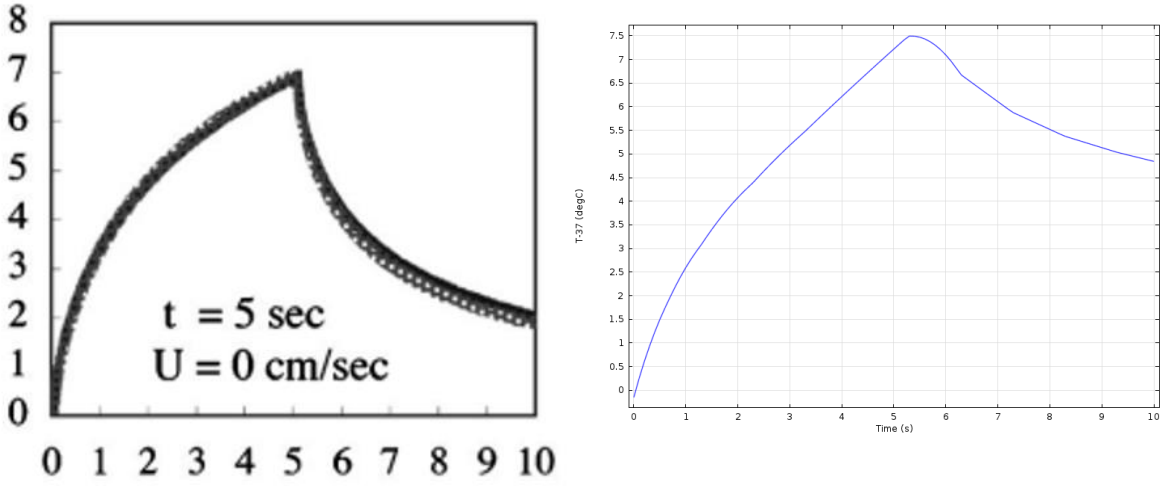

Figure 15. The temperature increase in the tissue after an insonation time of 5s at an ultrasound frequency of 1 MHz. The experimental results (left; from [23]) and the model results (right) both showed an increase of approximately 7 ºC after 5s of heating. The experiment and our model used the same water and tissue properties, surface intensity of 10^5 W/m^2, focal length of 62.64 mm, frequency of 1 MHz, and water temperature of 23 ºC.

Our study was computed for validation by using the same frequency, focal length, and initial water bath temperature, and the same order of magnitude of surface intensity values as those used in the experiment. The frequency was set at 1 MHz, the focal length was set at 62.64 mm, and the initial water bath temperature was set to room temperature of 23ºC. Our model used a surface intensity of 1.01×10^5 W/m^2, with a displacement amplitude of 41.5 nm. The experiment used a surface intensity of similar magnitude, 6.5×10^5 W/m^2.

Neither the experiment nor our model accounted for blood flow in the tissue. The initial temperature of the tumor and normal tissue was set at 37ºC. The pressure model was run for 5s, after which only the heat model was run to simulate removal of the transducer.

After ultrasound heating for 5s, the experiment showed a temperature increase of 7 ºC while our model showed a similar temperature increase of 7.5 ºC.

Any difference between our model and the experiment results is most likely due to a difference in the geometries. A more simplified geometry was used in the experiment. However, geometry may not have a significant effect on the results since both the experiment and our model measured temperature rise at a similar location and had the same focal length. The experiment and our model measured the temperature at the point of ultrasound focus, which led to similar temperature rise.

Conclusions

The results of our 2D model propose the optimal conditions for tumor destruction while preventing destruction to the surrounding normal breast tissue.

The initial model suggested that heating is highly dependent on ultrasound frequency; however, increasing frequency to 3 MHz did not result in focused heating of the tumor. Therefore, this justified the need to change the geometry in order to reach higher temperatures to focus heating in the tumor. Optimization was done for parameters of frequency and initial water bath temperature in order to achieve 100% tumor destruction and minimal normal breast tissue damage. The results indicated that the optimal conditions for tumor destruction include an ultrasound frequency of 2.75 MHz, an initial water temperature of 10 $°C$, and a heating time of 15 min. At these conditions, 100% of the tumor tissue reached 42 $°C$ for destruction, and only 4.18% (7.81 cm^3) reached 42 $°C$ and was damaged.

Currently, achieving complete removal of the tumor is one of the challenges of hyperthermia treatment [17]. Therefore, our model sought to and succeeded in achieving 100% of tumor destruction.

From sensitivity analysis, we can conclude that the average tumor temperature is not strongly sensitive to tissue and water thermal properties of density and specific heat. Therefore, variability in these thermal properties of tissue and water would not significantly affect the application time of the ultrasound treatment. However, greater sensitivity to attenuation in tissue as well as frequency-dependent surface intensity at the transducer justified the need to optimize frequency in our solution.

The model was compared to an *in vivo* experiment of hyperthermia ultrasound heating in tissue phantom. The comparison was done using a model with the same water and tissue properties, frequency, focal length, and water temperature, and similar surface intensity values as those in the experiment. A similar increase in temperature in the tumor after 5s of heating indicates that our model results are valid and can be applied to experimental conditions.

Design Constraints

Constraints to the model include tumor and tissue geometry, transducer geometry, cost, health and safety concerns, and patient comfort. The model assumes a perfectly spherical breast and tumor, which do not accurately reflect a real situation. In addition, variations in patient breast geometry and tumor size and location may alter treatment results. This model is also specific to a transducer of a certain geometry, focal length, and curvature. Therefore, the cost and construction of the particular transducer would become economic and manufacturing constraints.

In addition, health and safety is a major concern as healthy tissues must be protected. Cells can maintain homeostasis until approximately 40 °C [24]. At temperatures above 40 °C, cells become susceptible to damage. In order to minimize damage to healthy tissue, there may be limitations on the intensity and duration of ultrasound heating. Similarly,

greater patient comfort may be achieved via minimizing healthy tissue damage and shorter treatment.

Design Recommendations and Future Work

The results for our 2D model demonstrated that frequency, attenuation, thermal conductivity of tissue, and intensity of ultrasound had a significant effect on temperature increase. Properties such as specific heat and density did not affect average tumor temperature as much. For 100% ablation of breast tumors, we recommend optimizing the parameters of frequency and initial water temperature.

In terms of design, future work should include a 3D geometry of the breast tumor in order to model a more realistic geometry as well as using corresponding properties for the different layers of the breast, such as subcutaneous fat, gland tissue, and tumor tissue. An MRI or ultrasound image would generate an even more accurate and realistic model. Based on our results for acoustic pressure in the tissue and water domains, it was demonstrated that ultrasound could be focused with a circular transducer. However, the focal point of the pressure waves was not entirely within the area of maximum heating for our non-optimized models. In addition, some areas within the healthy tissue reached the ablation temperature of $42°C$. These results suggest that transducer geometry and placement can be further optimized in future work to allow for a better understanding of how various geometries relate to specific scenarios.

Furthermore, a future model could take into account additional techniques to protect the surrounding tissue while heating the tumor to a desired temperature. These include a moving transducer that can prevent constant heat generation in a single location, and also a cyclic ultrasound application in conjunction with intermittent periods of cooling by the surrounding water bath. In addition, another way to measure tissue heating is to evaluate t_{43}, the thermal dose in equivalent minutes at 43 ºC to determine the amount of thermal damage and necrosis to the tumor.

Implications and Relevance

The implications of our study may be applied in future research in and design of ultrasound hyperthermia cancer treatments. As therapeutic ultrasound currently gains popularity as an alternative non-invasive treatment option for breast cancer, our model provides a valuable understanding of the treatment parameters and their effects that can contribute to improving future therapies. Our study results also indicate the sensitivity of the tumor temperature to the applied frequency and the transducer geometry that determines the location of the ultrasound focal point in the tissue. Therefore, for optimal treatment with minimal damage to surrounding healthy tissues, the model suggests that custom treatment designs may be required for individual patients.

Furthermore, a greater understanding of the parameters of ultrasound hyperthermia allows the possibility of providing individualized treatment. Real geometries of the tumors and tissues of patients may be reconstructed using MRI, modeled using a software such as COMSOL, and analyzed in order to design custom treatments.

Finally, the model results are not limited to the context of breast tumor treatment. Since our sensitivity analysis shows that material properties, such as specific heat, thermal conductivity, and density of tissue, have little impact on the tumor temperature, the model also has relevance to patients diagnosed of cancer in different tissues and areas of the body. Therefore, the model is applicable to the ultrasound treatment of various cancers, and provides a convenient means of analyzing the potential side effects of different combinations of parameters used in treatment. Our study provides important insight that may contribute to research done in minimizing the side effects of and improving future ultrasound hyperthermia treatments.

APPENDIX A. Mathematical Statement of the Problem

Governing Equations

i. Heat Transfer

$$\rho C_p \frac{\partial T}{\partial t} = k\left[\frac{1}{r}\frac{\partial}{\partial r}\left[r\left(\frac{\partial T}{\partial r}\right)\right] + \frac{\partial^2 T}{\partial z^2}\right] + Q$$

ii. Helmholtz Equation for Pressure

$$\frac{1}{\rho_c}\left[\frac{1}{r}\frac{\partial}{\partial r}\left[r\left(\frac{\partial p}{\partial r}\right)\right] + \frac{\partial^2 p}{\partial z^2}\right] = \left(\frac{\omega}{c_c}\right)^2 \frac{p}{\rho_c}$$

Boundary Conditions

i. Heat Transfer

$T = optimized\ temperature\ (°C)\ at\ all\ water\ boundaries$
$T = 37°C\ at\ edge\ of\ normal\ tissue$

ii. Ultrasound Helmholtz Equation

$flux = -\omega^2 d_o$ at boundary of transducer and tissue
$flux = 0$ at all other boundaries

Initial Conditions

i. Heat Transfer

$T = 37°C\ for\ tumor\ and\ tissue$
$T = optimized\ temperature\ (°C)\ for\ water$

Definition of Variables and Parameters

Table A1. COMSOL variables and parameters.

Name	Variable	Value/Expression	Source
Transducer Heat Source $(\frac{W}{m^3})$	Q	$2\alpha_{ABS} I = 2\alpha \left\lvert Re\left(\frac{1}{2} pv\right)\right\rvert$	[8]
Acoustic Intensity Amplitude $\left(\frac{W}{m^2}\right)$	I	$I = \sqrt{{I_r}^2 + {I_c}^2 + {I_z}^2}$	[8]

Intensity in r direction $\left(\frac{W}{m^2}\right)$	I_r	$I_r = 0.5\lvert Re(pv_r)\rvert$	
Intensity in ϕ direction $\left(\frac{W}{m^2}\right)$	I_ϕ	$I_\phi = 0.5\lvert Re(pv_\phi)\rvert$	
Intensity in z direction $\left(\frac{W}{m^2}\right)$	I_z	$I_z = 0.5\lvert Re(pv_z)\rvert$	
Acoustic particle velocity in r direction $\left(\frac{m}{s}\right)$	v_r	$v_r = -\frac{\frac{\partial p}{\partial r}}{\rho_c i\omega}$	[8]
Acoustic particle velocity in ϕ direction $\left(\frac{m}{s}\right)$	v_ϕ	$v_\phi = -\frac{\frac{\partial p}{\partial \phi}}{\rho_c i\omega}$	
Acoustic particle velocity in z direction $\left(\frac{m}{s}\right)$	v_z	$v_z = -\frac{\frac{\partial p}{\partial z}}{\rho_c i\omega}$	
Frequency of Transducer (MHz)	f	Optimized	[8]
Angular velocity of transducer (rad/sec)	ω	$\omega = 2\pi f$	
Complex Density $\left(\frac{kg}{m^3}\right)$	ρ_c	$\rho_c = \rho\left(\frac{c}{c_c}\right)^2$	
Complex Speed of sound $\left(\frac{m}{s}\right)$	c_c	$\frac{\omega}{k\frac{\omega}{c} - i\alpha}$	[8]
Density of Water $\left(\frac{kg}{m^3}\right)$	ρ_{water}	Set as a function of temperature	[25]
Density of Tissue $\left(\frac{kg}{m^3}\right)$	ρ_{tissue}	1044	[8]
Speed of Sound in water $\left(\frac{m}{s}\right)$	c_{water}	1522	[18]
Speed of Sound in tissue $\left(\frac{m}{s}\right)$	c_{tissue}	1568	[8]
Specific Heat of water $\left(\frac{J}{kgK}\right)$	$C_{p,water}$	Set as a function of temperature	[19]
Specific Heat of tissue $\left(\frac{J}{kgK}\right)$	$C_{p,tissue}$	3710	[8]
Thermal conductivity of water $\left(\frac{W}{mK}\right)$	k_{water}	Set as a function of temperature	[16]
Thermal conductivity of	k_{tissue}	0.59	[8]

Tissue $\left(\frac{W}{mK}\right)$			
Attenuation dependence on Frequency for water $\left(\frac{Np}{m}\right)$	α_{water}	$\alpha_{0,water} * f^2$	[26]
Attenuation dependence on Frequency for tissue $\left(\frac{Np}{m}\right)$	α_{tissue}	$\alpha_{0,tissue} * f^{1.5}$	[27]
Attenuation coefficient of Water $\left(\frac{Np}{m/MHz}\right)$	$\alpha_{0,water}$	0.025	
Attenuation coefficient of Tissue $\left(\frac{Np}{m/Mhz}\right)$	$\alpha_{0,water}$	8.55	[8]
Intensity for validation $\left(\frac{W}{m^2}\right)$	I	$1.01 * 10^5$	[23]
Impedance for validation $\left(\frac{kg}{sec*m^2}\right)$	Z	$1.48 * 10^6$	[28]
Displacement amplitude of transducer (nm)	d_o	3.8 (non-optimized model & validation), 4.56 (optimized model)	[8]

APPENDIX B. Mesh Convergence Analysis

Mesh convergence was only done for the heat transfer portion of our model. For the pressure field portion, we chose a free triangular mesh of maximum size $\frac{c}{6f}$ in order to have mesh sizes on a smaller order of magnitude than the pressure waves' wavelength $\left(\lambda = \frac{c}{f}\right)$.

We chose free triangular elements for our mesh for heat transfer because our model involves curved surfaces such as the breast surface and tumor-breast interface. Interfaces between the domains required a finer mesh to account for fine temperature differences caused by variations in the pressure field; the focal center of the ultrasound (at the center of the tumor) also required a finer mesh.

We varied maximum element size, minimum element size, maximum element growth rate, and resolution of curvature, starting from the predefined settings for "Normal," "Fine," and so on, and decreasing the parameters for each successive mesh setting.

Figure A1 shows an example of a triangular mesh diagram with a predefined normal element size. The temperature at the center of the tumor was then plotted against time using various element size to find the point of convergence, which was at an element number of 81325.

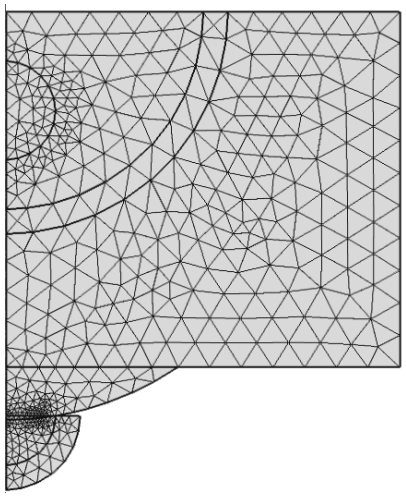

Figure A1. Free triangular mesh using predefined normal element size.

The mesh converged at 81325 elements (Figures A2, A3).

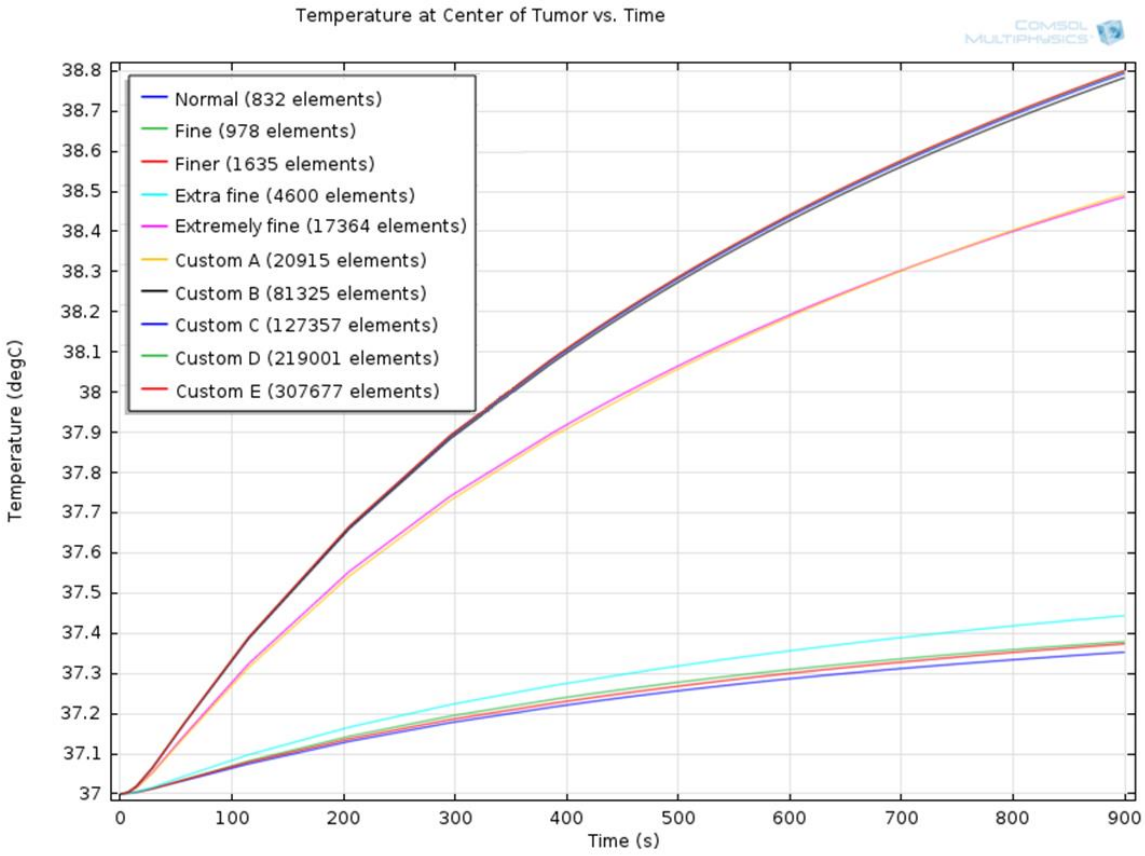

Figure A2. Temperature at the center of the tumor vs. time for different element sizes. Solutions of 81325 elements and above are extremely close (top four overlapping lines), indicating mesh convergence at 81325 elements.

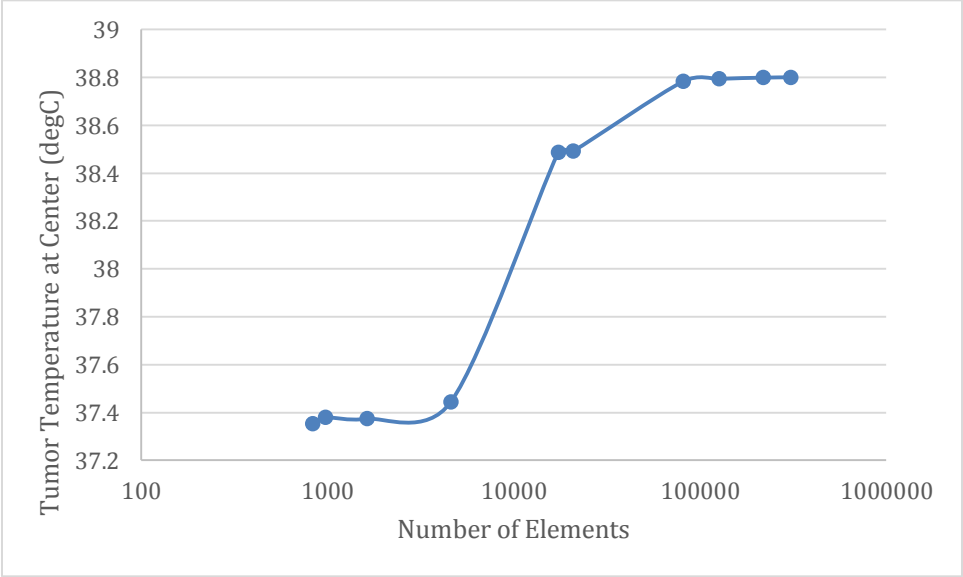

Figure A3. Temperature at the center of the tumor vs. number of mesh elements at 900s. The mesh converged at 81325 elements, as temperature appears to have stabilized.

APPENDIX C. Summary of Optimization Results

Frequencies between 1.5 MHz and 3.5 MHz were tested, along with combinations of initial water temperatures ranging from 10 °C to 35 °C.

We sought to find the conditions where, in order of priority:

1. All of the tumor was destroyed, by raising the entire tumor volume above 42 °C (necessary requirement).
2. As little of the normal tissue and fat were destroyed as possible, by keeping as much of the volume of normal tissue and fat below 42 °C.
3. The heating time was minimized.

The first item above is a necessary requirement. Thus, we found the time it takes for the entire tumor (100% of the volume) to reach 42 °C, for each combination of frequency and initial water temperature. Some conditions resulted in incomplete heating of the tumor within 15 minutes or less of treatment, indicated as "n/a" in Table A2 below.

We then found the percent of normal tissue that reached a temperature of 42 °C at the time found. The frequency and initial water temperature that resulted in the lowest amount of normal tissue damage, 4.18% (at a time of 900 seconds), was 2.75 MHz and 10 °C.

Table A2. Optimization results for tested conditions between 2 and 3 MHz and initial water temperatures between 10 and 35 °C.

Initial Water Temperature		**10 °C**		**15 °C**		**20 °C**		**25 °C**		**30 °C**		**35 °C**	
Fre-quency (MHz)	**Surface Intensity** (W/m^2)	% Normal Tissue Damage	Time (s)	% Normal Tissue Damage	Time (s)	% Normal Tissue Damage	Time (s)	% Normal Tissue Damage	Time (s)	% Normal Tissue Damage	Time (s)	% Normal Tissue Damage	Time (s)
1.5	2733.6	n/a	n/a	n/a	n/a	n/a	n/a	n/a	n/a	n/a	n/a	n/a	n/a
2	4859.7	n/a	n/a	n/a	n/a	n/a	n/a	0.0421	750	0.0750	630	0.1347	600
2.25	6150.6	n/a	n/a	n/a	n/a	n/a	n/a	0.0553	840	0.1012	750	0.1647	690
2.5	7593.3	n/a	n/a	0.0495	630	0.0751	600	0.1065	570	0.1463	540	0.2044	540
2.75	9187.9	0.0418	900	0.0668	720	0.0950	660	0.1307	630	0.1726	600	0.2212	570
3	10934.4	n/a	n/a	n/a	n/a	0.1057	840	0.1437	750	0.1920	720	0.2437	690
3.5	14882.9	n/a	n/a	n/a	n/a	n/a	n/a	n/a	n/a	n/a	n/a	n/a	n/a

APPENDIX D. References

[1] J. M. Allen, "Economic/societal burden of metastatic breast cancer: a US perspective," *Am J Manag Care*, vol. 16, pp. 697-704, Sep 2010.

[2] American Cancer Society. (2013, February 13, 2013). *Hyperthermia to treat cancer*. Available: http://www.cancer.org/treatment/treatmentsandsideeffects/treatmenttypes/hyperthermia

[3] P. E. Huber, *et al.*, "A New Noninvasive Approach in Breast Cancer Therapy Using Magnetic Resonance Imaging-guided Focused Ultrasound Surgery," *Cancer Research*, vol. 61, pp. 8441-8447, 2001.

[4] B. A. Grotenhuis, *et al.*, "Radiofrequency ablation for early-stage breast cancer: Treatment outcomes and practical considerations," *European Journal of Surgical Oncology (EJSO)*, vol. 39, pp. 1317-1324, 2013.

[5] W. G. Pitt, *et al.*, "Ultrasonic drug delivery--a general review," *Expert Opin Drug Deliv*, vol. 1, pp. 37-56, Nov 2004.

[6] S. Thuroff, *et al.*, "High-intensity focused ultrasound and localized prostate cancer: efficacy results from the European multicentric study," *J Endourol*, vol. 17, pp. 673-7, Oct 2003.

[7] D. Gianfelice, *et al.*, "Feasibility of magnetic resonance imaging-guided focused ultrasound surgery as an adjunct to tamoxifen therapy in high-risk surgical patients with breast carcinoma," *J Vasc Interv Radiol*, vol. 14, pp. 1275-82, Oct 2003.

[8] COMSOL. (2013, February 12, 2014). *Focused ultrasound induced heading in tissue phantom*. Available: http://www.comsol.com/model/focused-ultrasound-induced-heating-in-tissue-phantom-12659

[9] L. Merckel, *et al.*, "MR-Guided High-Intensity Focused Ultrasound Ablation of Breast Cancer with a Dedicated Breast Platform," *CardioVascular and Interventional Radiology*, vol. 36, pp. 292-301, 2013/04/01 2013.

[10] J. E. Kennedy, "High-intensity focused ultrasound in the treatment of solid tumours," *Nat Rev Cancer*, vol. 5, pp. 321-327, 2005.

[11] F. K. Storm, *et al.*, "Normal tissue and solid tumor effects of hyperthermia in animal models and clinical trials," *Cancer Res*, vol. 39, pp. 2245-51, Jun 1979.

[12] S. R. Guntur, *et al.*, "Temperature-Dependent Thermal Properties of ex Vivo Liver Undergoing Thermal Ablation," *Ultrasound in Medicine & Biology*, vol. 39, pp. 1771-1784, 2013.

[13] F. J. González. (2011, December 1, 2011). Non-invasive estimation of the metabolic heat production of breast tumors using digital infrared imaging. *ArXiv e-prints 1112*, 2173. Available: http://adsabs.harvard.edu/abs/2011arXiv1112.2173G

[14] M. Mital and R. M. Pidaparti, "Breast Tumor Simulation and Parameters Estimation Using Evolutionary Algorithms," *Modelling and Simulation in Engineering*, vol. 2008, 2008.

[15] O. M. Hassan, *et al.*, "Modeling of ultrasound hyperthermia treatment of breast tumors," in *Radio Science Conference, 2009. NRSC 2009. National*, 2009, pp. 1-8.

[16] C. A. Nieto de Castro, *et al.*, "Standard Reference Data for the Thermal Conductivity of Liquids," *Journal of Physical and Chemical Reference Data,* vol. 15, pp. 1073-1086, 1986.
[17] S. Li and P. H. Wu, "Magnetic resonance image-guided versus ultrasound-guided high-intensity focused ultrasound in the treatment of breast cancer," *Chin J Cancer,* vol. 32, pp. 441-52, Aug 2013.
[18] N. Bilaniuk and G. S. K. Wong, "Speed of sound in pure water as a function of temperature," *J Acoust Soc Am,* vol. 93, pp. 1609-1612, 1993.
[19] J. Osborne, Stimson, M, Ginnings, S, *Handbook of chemistry and physics*, 53rd ed. Cleveland, OH: Chemical Rubber Company, 1972.
[20] G. Ghoshal, *et al.*, "Temperature dependent ultrasonic characterization of biological media," *J Acoust Soc Am,* vol. 130, pp. 2203-11, Oct 2011.
[21] A. Bhattacharya and R. L. Mahajan, "Temperature dependence of thermal conductivity of biological tissues," *Physiol Meas,* vol. 24, pp. 769-83, Aug 2003.
[22] D. Haemmerich, *et al.*, "In vitro measurements of temperature-dependent specific heat of liver tissue," *Med Eng Phys,* vol. 28, pp. 194-7, Mar 2006.
[23] J. Huang, *et al.*, "Experimental validation of a tractable numerical model for focused ultrasound heating in flow-through tissue phantoms," *J Acoust Soc Am,* vol. 116, pp. 2451-8, Oct 2004.
[24] S. N. Goldberg, *et al.*, "Thermal ablation therapy for focal malignancy: a unified approach to underlying principles, techniques, and diagnostic imaging guidance," *AJR Am J Roentgenol,* vol. 174, pp. 323-31, Feb 2000.
[25] W. M. Haynes, "CRC Handbook of Chemistry and Physics," 94th ed Boca Raton, FL: CRC Press/Taylor and Francis, 2014.
[26] L. Mordfin, "Handbook of Reference Data for Nondestructive Testing," ed West Conshohocken, PA: ASTM International, 2002, p. 41.
[27] F. T. D'Astous and F. S. Foster, "Frequency dependence of ultrasound attenuation and backscatter in breast tissue," *Ultrasound Med Biol,* vol. 12, pp. 795-808, Oct 1986.
[28] H. Azhari, "Appendix A: Typical Acoustic Properties of Tissues," in *Basics of Biomedical Ultrasound for Engineers,* ed: John Wiley & Sons, Inc., 2010, pp. 313-314.